CONF-860421--31

CONF-860421--31

DE86 010396

MODIFICATION OF THE GRAIN BOUNDARY MICROSTRUCTURE OF THE AUSTENITIC PCA STAINLESS STEEL TO IMPROVE HELIUM EMBRITTLEMENT RESISTANCE*

P. J. Maziasz and D. N. Braski

Metals and Ceramics Division, Oak Ridge National Laboratory,
P. O. Box X, Oak Ridge, TN 37831

Abstract

Grain boundary MC precipitation was produced by a modified thermal-mechanical pretreatment in 25% cold worked (CW) austenitic prime candidate alloy (PCA) stainless steel prior to HFIR irradiation. Postirradiation tensile results and fracture analysis showed that the modified material (B3) resisted helium embrittlement better than either solution annealed (SA) or 25% CW PCA irradiated at 500 to 600°C to ~21 dpa and 1370 at. ppm He. PCA SA and 25% CW were not embrittled at 300 to 400°C. Grain boundary MC survives in PCA-B3 during HFIR irradiation at 500°C but dissolves at 600°C; it does not form in either SA or 25% CW PCA during similar irradiation. The grain boundary MC appears to play an important role in the helium embrittlement resistance of PCA-B3.

---

*Research sponsored by the Office of Fusion Energy, U.S. Department of Energy, under Contract DE-AC05-84OR21400 with the Martin Marietta Energy Systems, Inc.

1.0 Introduction

Recent articles discuss current work and provide perspective on the general problem of helium embrittlement in austenitic stainless steels [1–4]. The problem is expected to be quite severe above 550 to 600°C at the high helium generation rates to be found in a fusion reactor first wall. However, at temperatures in the 400 to 600°C range, high swelling is the most severe problem limiting lifetime. Helium embrittlement imposes lifetime limits only when the steel is already resistant to void swelling [4].

The PCA is a 14Cr–16Ni–2.5Mo–0.25Ti–0.4Si–0.05C (all in weight percent) austenitic stainless steel whose composition was developed for void swelling resistance [5]. However, for fusion application with high helium generation rates, neither swelling nor embrittlement resistance are indigenous properties of an alloy. Instead, both properties depend on preirradiation microstructural condition. A variety of preirradiation microstructures of PCA have been evaluated after HFIR irradiation [3,6,7]. Swelling resistance was found to be optimum in heavily (20–25%) cold worked material [7]. Matrix MC, either coarse or fine, introduced via thermal pretreatments dissolves at 500 to 600°C. By contrast, preaging to produce moderately coarse (10–70 nm in diameter) grain boundary MC was the only method to improve embrittlement resistance in HFIR-irradiated PCA [3]. The formation and stability of MC are vital to both embrittlement and void swelling resistance in steels. Stability is only one facet of the more general understanding of precipitation behavior in irradiated steels that has developed recently [4,8].

Previous work showed embrittlement resistance qualitatively via disk-bend testing, but did not combine optimum pretreatments for swelling and

embrittlement resistance together. Therefore, the objective of this work is to evaluate the swelling and embrittlement resistance of a new, optimized microstructural variant of PCA, designated B3. The B3 microstructure consists of medium-coarse (10–70 nm diam) grain boundary MC particles, produced by aging of SA material prior to cold working. Mechanical properties were evaluated quantitatively by postirradiation tensile testing of larger, bar-type specimens.

2.0 Experimental

The PCA was fabricated into 5-mm-diam rod stock in either the 25% CW (A3), the B3, or the 50% CW condition. The B3 material was solution annealed for 30 min at 1100°C, aged at 800°C for 8 h, and then cold worked 25%. Standard HFIR "sub-mini" buttonhead tensile specimens (gage lengths - 18.3 mm, gage diam - 2 mm) were machined from rod stock. The 50% CW specimens were then annealed for 30 min at 1100°C to produce the SA (A1) microstructure.

Specimens were irradiated in experiments HFIR-CTR-42 and -43. Elevated temperatures were achieved by nuclear heating and controlled via insulating gas gaps that kept irradiation temperatures uniform over the shoulder and gage regions of the specimens. Irradiation temperatures of 300, 400, 500, and 600°C were calculated, based on recent temperature measurements from similar gas-gap experiments [9]. Specimens accumulated neutron fluences producing 16.6 to 20.8 dpa and 1060 to 1371 at. ppm He, based on dosimetry and calculations by Greenwood [10].

The irradiated specimens were tensile tested in a hot cell in an INSTRON universal testing machine at the irradiation using a strain rate

of 0.51 mm/min. Unirradiated controls were tested at 300, 500, and 600°C while aged PCA-A3 and B3 specimens (5000 h at 600°C) were tested at 600°C.

Transmission electron microscopy (TEM) disks were sliced from the shoulders of several tested HFIR specimens and thinned via a remotely controlled TENUPOL unit. The disks were examined using a JEM 2000FX analytical electron microscope (AEM). Fractography was performed on a modified AMRAY 1200B scanning electron microscope (SEM), also installed in a hot cell.

3.0 Results

3.1 Tensile Properties

Irradiation in HFIR at 300 and 400°C produced considerable hardening, whereas there was less hardening at 500°C, and little or none at 600°C. Tensile properties for HFIR-irradiated specimens are listed in Table 1 and shown graphically with the unirradiated control data in Fig. 1. (The tensile properties of the control specimens are listed elsewhere [11,12].) The PCA-A1 was softest prior to irradiation and experienced the most strengthening during irradiation. The PCA-A1, -A3, and -B3 all approached similar strength after irradiation, but PCA-A3 was slightly stronger than the others. Unirradiated PCA-B3 was the strongest material at 500 and 600°C. Irradiation caused PCA-A1 and -A3 to have high (900–1000 MPa), equal values of yield and ultimate tensile strength (YS and UTS, respectively) at 300 and 400°C. The YS and UTS were measurably different from each other in PCA-A3 and -B3 at 500 and 600°C, but they still were nearly equal for PCA-A1.

Irradiation caused significant ductility losses in all specimens except PCA-B3, which actually had better ductility after irradiation at 500°C than unirradiated material (Fig. 1). The PCA-A1, which had the most

ductility prior to irradiation, had the lowest ductility after irradiation. Ductility losses of PCA-A1 and -A3 at 300 and 400°C correlated reasonably well with general increases in strength caused by irradiation hardening. But progressively greater ductility losses at 500 and 600°C despite decreases in strength suggested that helium was embrittling both of these materials. Total elongation (TE) decreased with temperature for PCA-A1, from ~7% at 300°C to 0.6% at 600°C. Uniform elongation (UE), however, was very low (0.1–0.3%) at 300 and 400°C, and reached a maximum (1.4%) at 500°C and then became low (0.3%) again at 600°C. Ductility behavior with temperature for both PCA-A1 and -A3 was parallel but the PCA-A1 was less ductile.

In contrast to PCA-A1 or -A3, PCA-B3 appeared to resist helium embrittlement somewhat better than the others at 600°C and to resist it entirely at 500°C. At 500°C, the UE of B3 was low prior to irradiation, making its increase during irradiation quite significant. After irradiation at 600°C, UTS decreased while UE again increased. Aging at 600°C decreased the UE of unirradiated PCA-A3, whereas aging increased it for PCA-B3. Although PCA-B3 showed some signs of helium embrittlement at 600°C, it was not as severe as observed in PCA-A1 or -A3.

3.2 SEM - Fracture Analysis

Unirradiated control specimens generally fractured via a ductile dimple-type failure mode up to 600°C. However, after HFIR irradiation at 600°C, fracture became intergranular to varying degrees, depending upon alloy pretreatment. PCA-A3 failed intergranularly across the entire gage after irradiation at 600°C, whereas PCA-B3 showed a mixture of ductile-transgranular and intergranular failure modes. After irradiation at 500°C, the failure mode was ductile shear in the middle of the gage cross section

for all samples, but varied near the outer edge. As shown in Fig. 2, PCA-B3 failed in a ductile mode at the specimen edge, whereas in PCA-A1, the failure was intergranular. In spite of low ductilities after irradiation at 400°C, specimens failed in a ductile-dimple mode, similar to unirradiated material.

3.3 TEM - Microstructural Analysis

Specimens for microstructural examination were taken from the shoulders of PCA-A1 and -B3 tensile specimens irradiated at 500 and 600°C. Previous work showed that HFIR irradiation at 300 and 400°C to 44 dpa produced similar microstructures with many Frank loops and fine bubbles in alloys with various pretreatments, including PCA-A1, and -A3. However, microstructural evolution varied considerably with pretreatment at higher temperatures [3,7].

The PCA-B3 had many fine bubbles in the matrix after irradiation at 500 and 600°C to ~20 dpa, and possibly a few voids at 500°C. The amount of fine irradiation-produced MC (1—10 nm in diam) increased with temperature, whereas dislocation and loop concentrations decreased. Compared to PCA-B3, A1 had many large voids together with fewer and somewhat coarser bubbles at 500 and 600°C. The PCA-A1 material also had more large loops and less MC with the additional formation of G and γ' phases. The PCA-B3 microstructures were very similar to those found previously in HFIR irradiations of PCA-A3 at 500 and 600°C to 22 dpa [3].

PCA-B3 contained intergranular MC precipitation (10—70 nm in diam) after irradiation at 500°C to ~20 dpa, whereas PCA-A1 did not (see Figs. 3 and 4). The grain boundary MC produced in PCA-B3 prior to irradiation remained stable at 500°C, but not at 600°C. Some coarse grain boundary

$M_6C(\eta)$ [and/or $M_{23}C_6$ (τ) or G] precipitated sporadically at 500°C in PCA-B3, but more frequently at 600°C. Similar coarse particles were more abundant in PCA-Al at 500°C than at 600°C [see Fig. 3(a) and (b)]. Bubbles were larger and more concentrated in the precipitate-free grain boundaries in PCA-Al than in PCA-B3, particularly at 500°C [see Fig. 3(c) and (d)]. Many of the finer bubbles in PCA-B3 were attached to MC particles in the boundary. At 600°C, however, grain boundary regions in PCA-B3 that experienced MC dissolution were similar to those in PCA-Al.

Finally, we note that grain boundary regions were poorly defined in PCA-Al at 500°C. Details suggest that the grain boundaries may have migrated and swept up helium bubbles, leaving trails of elongated precipitates and voids behind. Grain boundary regions are better defined and apparently more stable in PCA-B3.

4.0 Discussion

For this experiment, microstructures and properties correlate quite well. Loops appear to be the major source of matrix hardening, because temperature and pretreatment effects on strength correlated with their effects on Frank loop formation and stability. At 600°C it appears that fine MC particles and possibly bubbles pin the network dislocations to strengthen PCA-A3 and -B3 relative to -Al. At grain boundaries of PCA-Al and -A3, coarser helium bubbles and lack of precipitation contribute to helium embrittlement at 500 and 600°C. Conversely, MC and bubble refinement at grain boundaries contribute to the embrittlement resistance of PCA-B3.

Comparison with previous HFIR data at less than 20 dpa [13–15] shows that the YS of the 25% CW PCA was 100 to 200 MPa stronger than 20% CW 316 or 316+Ti stainless steels, while SA PCA was 200 to 300 MPa stronger than

the same SA steels at 400 to 600°C. However, SA and 25% CW PCA were less ductile, particularly between 500 and 600°C.

The helium embrittlement resistance of PCA-B3 at 500 and 600°C was consistent with qualitative disk-bend testing on two pretreatment variants of PCA with similar grain boundary MC precipitation [3]. The embrittlement behavior of PCA-A1 and -A3 at 400 to 600°C was also qualitatively consistent with those bend test results.

There are several effects of grain boundary MC to consider in explaining its role in helium embrittlement resistance during neutron irradiation: (a) the effect of MC particles trapping helium, producing a refined bubble distribution at their interfaces, (b) the effects of the MC precipitation on grain-boundary behavior, and (c) the stability of the MC particles. In the first effect, if embrittlement is related to critical bubble size at the grain boundaries [16], then the benefits of MC to refine and pin bubbles to hinder their growth or coalescence are obvious. The second and third effects are related. The oversized MC particles themselves may alter the sink nature of the grain boundary for helium as well as prevent boundary migration and sweeping. However, all benefits disappear if the MC becomes unstable due to segregation processes in the matrix [5]. Schroeder et al. [1] and Kesternich [2] identify MC stability during neutron irradiation as a key "open" issue. We believe that the present results provide some new information concerning the limits of MC stability during irradiation.

Finally, Schroeder et al. [1] and Kesternich [2] suggest that embrittlement resistance stems from the helium trapping of fine matrix MC particles, based on helium injection and thermal creep data. Our work suggests

that helium embrittlement resistance depends more on MC particles within grain boundaries. Similar dispersions of fine matrix MC and bubbles form in PCA-A3 and -B3 in HFIR, but better helium embrittlement resistance correlates with the grain boundary MC present in PCA-B3. While both mechanisms appear valid, further experiments are needed to evaluate both of them at in-reactor creep conditions relevant to fusion.

5.0 Conclusions

Helium embrittlement is not a problem in HFIR at 300 and 400°C after ~19 dpa and 1230 at. ppm He, as PCA-A1 and -A3 become very strong but fail in a ductile manner. They do, however, become progressively more embrittled with increasing temperature at 500 and 600°C due to helium.

PCA-B3 is more resistant to helium embrittlement than either PCA-A1 or -A3 after HFIR irradiation at 500 and 600°C. At 500°C, irradiation actually improves the ductility. The embrittlement resistance appears directly related to the effects and stability of grain boundary MC produced by aging prior to irradiation.

References

[1] H. Schroeder, W. Kesternich, and H. Ullmaier, Nucl. Engin. and Design/Fusion 2 (1985) 65–95.

[2] W. Kesternich, J. Nucl. Mater. 127 (1985) 153–160.

[3] P. J. Maziasz and D. N. Braski, J. Nucl. Mater. 122 and 123 (1984) 305–310.

[4] P. J. Maziasz, J. Nucl. Mater. 133 and 134 (1985) 134–140.

[5] P. J. Maziasz, J. Nucl. Mater. 122 and 123 (1984) 472–486.

[6] P. J. Maziasz and T. K. Roche, J. Nucl. Mater. 103 and 104 (1981) 797–802.

[7] P. J. Maziasz and D. N. Braski, J. Nucl. Mater. 122 and 123 (1984) 311–316.

[8] E. H. Lee, P. J. Maziasz and A. F. Rowcliffe, pp. 191–278 in: Conf. Proc. Phase Stability Under Neutron Irradiation, TMS-AIME, 1981.

[9] M. L. Grossbeck, J. W. Woods, and G. A. Potter, pp. 36–44 in: ADIP Quart. Prog. Rept., DOE/ER-0045/4 (1980) Office of Fusion Energy, U.S. Department of Energy.

[10] L. R. Greenwood, pp. 13–17 in: ADIP Semiannu. Prog. Rept., DOE/ER-0045/13 (1984) Office of Fusion Energy, U.S. Department of Energy.

[11] D. N. Braski and P. J. Maziasz, J. Nucl. Mater. 122 and 123 (1984) 338-342.

[12] D. N. Braski and P. J. Maziasz, pp. 61–63 in: ADIP Semiannu. Prog. Rept., DOE/ER-0045/12 (1984) Office of Fusion Energy, U.S. Department of Energy.

[13] M. L. Grossbeck and P. J. Maziasz, pp. 32–49 in: ADIP Quart. Prog. Rept., DOE-ER-0058/3 (1978) Office of Fusion Energy, U.S. Department of Energy.

[14] M. L. Grossbeck and P. J. Maziasz, J. Nucl. Mater. 103 and 104 (1981) 827–832.

[15] R. L. Klueh and M. L. Grossbeck, pp. 768–782 in: Effects of Radiation on Materials, Twelfth Inter. Symp., ASTM-STP-870, Amer. Soc. for Testing and Matls., Philadelphia, PA, 1985.

[16] G. R. Odette, J. Nucl. Mater. 122 and 123 (1984) 435–441.

Table 1. Postirradiation tensile data for PCA irradiated in HFIR

Material condition	Irradiation temperature (°C)	Conditions[a]			Strength,[b] MPa		Elongation, %	
		Fluence ($\times 10^{26}$ n/m^2) (E > 0.1 MeV)	Displacement damage (dpa)	Helium level (at. ppm)	Yield	Ultimate	Uniform	Total
PCA-B3	600	2.46	20.8	1370	508	579	3.2	3.8
PCA-A3	600	2.40	20.3	1335	539	570	1.0	1.1
PCA-A3	600	2.40	20.3	1335	513	548	1.2	1.7
PCA-A1	600	2.46	20.8	1370	468	473	0.3	0.6
PCA-B3	500	2.40	20.3	1335	659	745	5.3	8.6
PCA-A3	500	2.25	19.0	1234	692	771	3.4	6.2
PCA-A3	500	2.25	19.0	1234	767	842	2.0	3.9
PCA-A1	500	2.40	20.3	1335	765	793	1.4	3.3
PCA-A3	400	1.97	16.6	1060	950	951	0.2	4.4
PCA-A3	400	2.25	19.0	1234	935	938	0.3	4.1
PCA-A3	400	1.97	16.6	1060	976	980	0.3	4.1
PCA-A1	400	2.25	19.0	1234	896	897	0.1	5.5
PCA-A3	300	1.97	16.6	1060	973	973	0.2	5.3
PCA-A1	300	1.97	16.6	1060	851	851	0.3	7.3

[a]Displacement damage and helium were calculated from dosimetry measurements made by Greenwood [10].

[b]Specimens were tested at the irradiation temperature.

Figure Captions

Fig. 1. Plots of yield and ultimate tensile stress and uniform and total elongation, respectively, for PCA-A1 (a,d), PCA-A3 (b,e) and PCA-B3 (c,f) as functions of test temperatures. HFIR irradiated specimens were tested at their irradiation temperatures. Data on unirradiated control specimens and specimens aged for 5000 h at 600°C are included for comparison from [12].

Fig. 2. SEM of fractures for (a) PCA-A1 (EJ-6) and (b) PCA-B3 (EL-7) irradiated in HFIR at 500°C to 20.3 dpa and 1335 at. ppm He. PCA-A1 shows some intergranular failure near the specimen surface where PCA-B3 shows ductile-shear failure throughout the gage cross section.

Fig. 3. TEM comparison of grain boundary MC precipitation via dark-field imaging for PCA-B3 (a) as-heat-treated prior to irradiation and (b) after HFIR irradiation at 500°C to 20.3 dpa and 1335 at. ppm He. Most of the MC particles survive during irradiation, despite some coarsening and/or dissolution.

Fig. 4. TEM comparison of grain boundary precipitation at lower magnification (a,b) and grain boundary helium bubbles at higher magnification (c,d) for PCA-A1 (a,c) and -B3 (b,d) irradiated in HFIR at 500°C to 20.3 dpa and 1335 at. ppm He. Note the fine bubbles attached to MC particles in PCA-B3 (d).

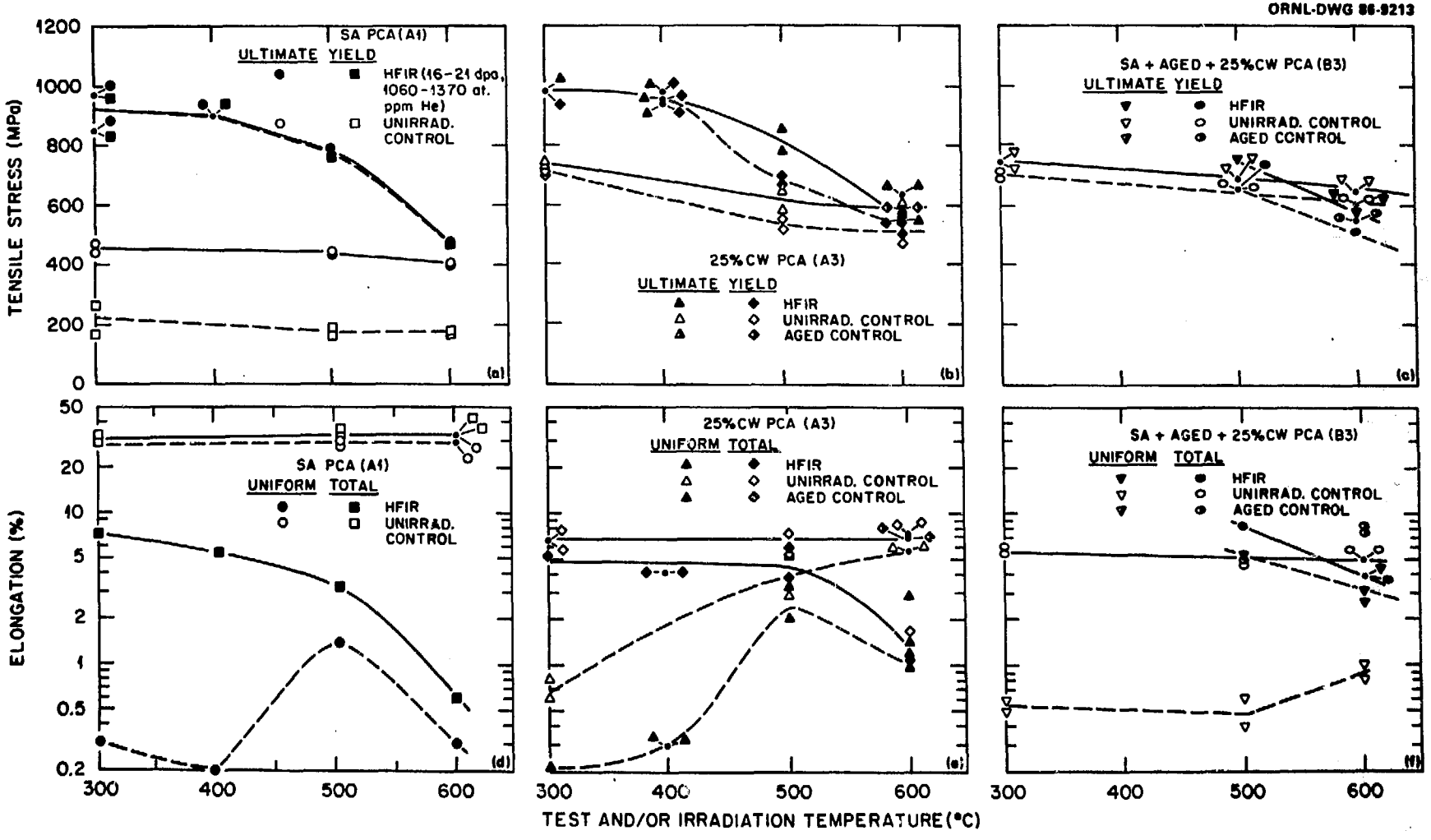
ORNL-DWG 86-9213
SA PCA (A1)
ULTIMATE YIELD
HFIR (16-21 dpa, 1060-1370 at. ppm He)
UNIRRAD. CONTROL
25%CW PCA (A3)
ULTIMATE YIELD
HFIR
UNIRRAD. CONTROL
AGED CONTROL
SA + AGED + 25%CW PCA (B3)
ULTIMATE YIELD
HFIR
UNIRRAD. CONTROL
AGED CONTROL
SA PCA (A1)
UNIFORM TOTAL
HFIR
UNIRRAD. CONTROL
25%CW PCA (A3)
UNIFORM TOTAL
HFIR
UNIRRAD. CONTROL
AGED CONTROL
SA + AGED + 25%CW PCA (B3)
UNIFORM TOTAL
HFIR
UNIRRAD. CONTROL
AGED CONTROL
TENSILE STRESS (MPa)
ELONGATION (%)
TEST AND/OR IRRADIATION TEMPERATURE (°C)
1200
1000
800
600
400
200
0
50
20
10
5
2
1
0.5
0.2
300
400
500
600
(a)
(b)
(c)
(d)
(e)
(f)

Fig 1

PCA-B3 SHOWS ENTIRELY DUCTILE SHEAR

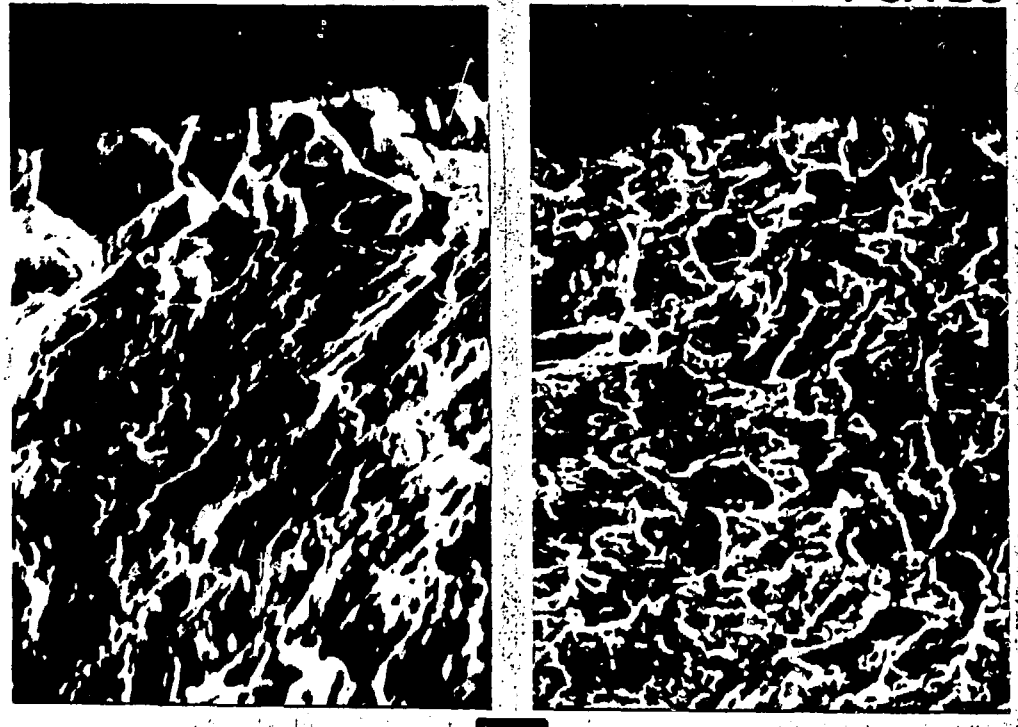

- HFIR, 500°C, 20.3 dpa, 1335 at. ppm He
- TENSILE TESTED AT 500°C

HFIR

- HFIR, 400°
- TENSILE T

Fig. 2

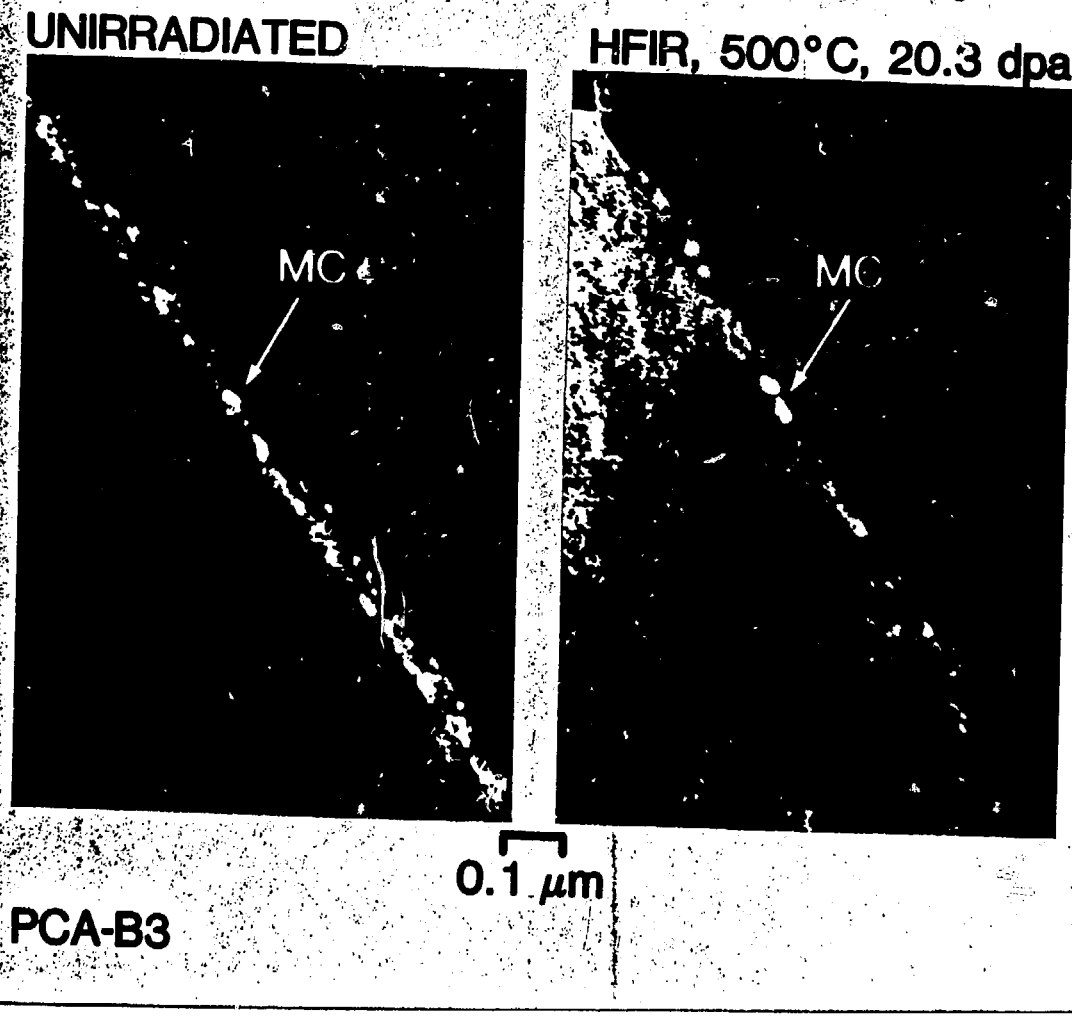

Fig. 3

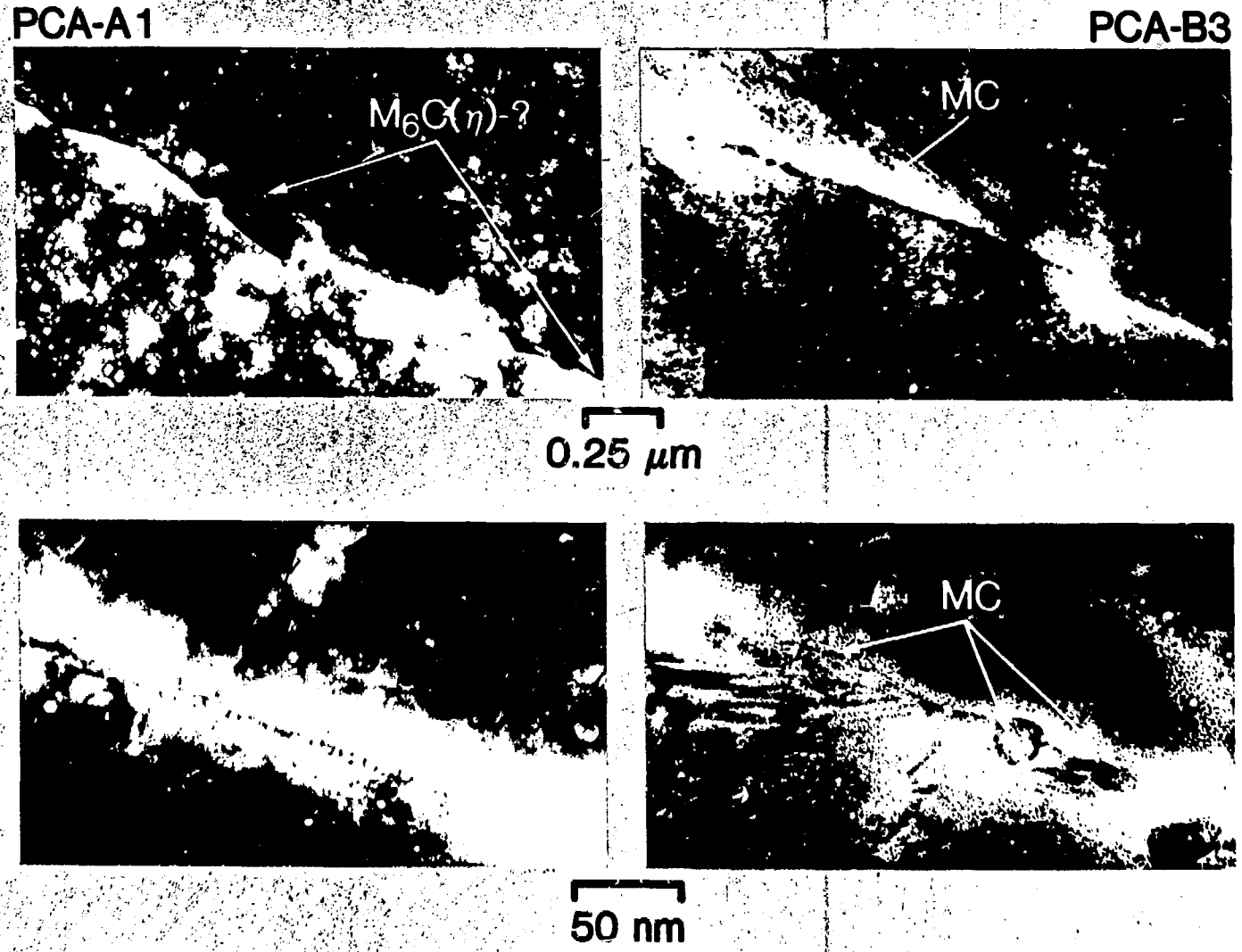

Fig. 4